



OPEN

Design, synthesis, molecular docking study, and α -glucosidase inhibitory evaluation of novel hydrazide–hydrazone derivatives of 3,4-dihydroxyphenylacetic acid

Hammad Khan¹, Faheem Jan^{2,3}, Abdul Shakoore⁴, Ajmal Khan⁵, Abdullah F. AlAsmari⁶, Fawaz Alasmari⁶, Saeed Ullah⁵, Ahmed Al-Harrasi^{5✉}, Momin Khan^{4✉} & Shaukat Ali^{1✉}

A series of novel Schiff base derivatives (1–28) of 3,4-dihydroxyphenylacetic acid were synthesized in a multi-step reaction. All the synthesized Schiff bases were obtained in high yields and their structures were determined by ¹HNMR, ¹³CNMR, and HR-ESI-MS spectroscopy. Except for compounds 22, 26, 27, and 28, all derivatives show excellent to moderate α -glucosidase inhibition. Compounds 5 (IC₅₀ = 12.84 ± 0.52 μ M), 4 (IC₅₀ = 13.64 ± 0.58 μ M), 12 (IC₅₀ = 15.73 ± 0.71 μ M), 13 (IC₅₀ = 16.62 ± 0.47 μ M), 15 (IC₅₀ = 17.40 ± 0.74 μ M), 3 (IC₅₀ = 18.45 ± 1.21 μ M), 7 (IC₅₀ = 19.68 ± 0.82 μ M), and 2 (IC₅₀ = 20.35 ± 1.27 μ M) shows outstanding inhibition as compared to standard acarbose (IC₅₀ = 873.34 ± 1.67 μ M). Furthermore, a docking study was performed to find out the interaction between the enzyme and the most active compounds. With this research work, 3,4-dihydroxyphenylacetic acid Schiff base derivatives have been introduced as a potential class of α -glucosidase inhibitors that have remained elusive till now.

Diabetes mellitus is a persistent and potentially life-threatening metabolic condition characterized by inadequate insulin secretion, resulting in a complication known as hyperglycaemia^{1–4}. In type II diabetes mellitus, linked to increased postprandial glucose levels, there is an elevated risk of stroke, atherosclerosis, and other cardiovascular conditions^{5,6}. Therefore, an effective approach to managing type II diabetes mellitus and its associated issues involves the inhibition of digestive enzymes, specifically aimed at alleviating postprandial hyperglycemia^{7–9}. As enzyme activity and blood glucose concentrations are strongly correlated with each other, the inhibition of α -glucosidase can potentially decrease postprandial blood glucose levels^{10,11}. The function of α -glucosidase inhibitors like acarbose, miglitol, and voglibose, used in clinical settings is to slow down sharp rises in blood sugar levels^{12,13}. The α -glucosidase enzyme found in human intestinal cells serves a crucial role as the primary hydrolase enzyme. Its primary function involves breaking down complex carbohydrates into glucose monomers, which can then readily diffuse into the bloodstream^{14,15}. In the case of type II diabetes, where human body is resistant to insulin then α -glucosidase inhibitors utilization plays a beneficial role in reducing postprandial hyperglycaemia^{16,17}. Commonly available α -glucosidase inhibitors such as acarbose, miglitol, and voglibose are associated with side effects such as diarrhea, nausea, and other intestinal disturbances^{18,19}. Notably, numerous pieces of evidences indicate that α -glucosidase inhibitors may prove beneficial in the treatment of carbohydrate-mediated diseases, including conditions such as cancer, Alzheimer's disease, hepatitis, and bacterial and viral infections^{20–22}. Consequently use of α -glucosidase inhibitors has emerged as a promising therapeutic avenue for mitigating the risks associated with diabetes and related conditions^{23,24}. Therefore, the pursuit of designing

¹Organic Synthesis and Catalysis Research Laboratory, Institute of Chemical Sciences, University of Peshawar, Peshawar 25120, Khyber Pakhtunkhwa, Pakistan. ²Shenyang National Laboratory for Materials Science, Institute of Metal Research Chinese Academy of Sciences, Shenyang 110016, Liaoning, China. ³School of Materials Science and Engineering, University of Science and Technology of China, Shenyang 110016, Liaoning, China. ⁴Department of Chemistry, Abdul Wali Khan University, Mardan 23200, Pakistan. ⁵Natural and Medical Sciences Research Center, University of Nizwa, PO Box 33, 616 Birkat Al Mauz, Nizwa, Oman. ⁶Department of Pharmacology and Toxicology, College of Pharmacy, King Saud University, Riyadh 11451, Saudi Arabia. ✉email: aharrasi@unizwa.edu.om; mominkhan@awkum.edu.pk; drshaukatali@uop.edu.pk

and developing novel α -glucosidase inhibitors with high efficacy and minimal side effects holds a great appeal for medicinal chemists.

Schiff bases are one of the most widely used organic compounds having a broad range of applications in different fields such as biology, medicinal drugs, organometallic chemistry, inorganic and analytical chemistry^{25–32}. Imine or azomethine groups in Schiff bases has shown profound biological importance and have been recognized as privileged precursors for designing biologically active drugs^{36–38} with a broad spectrum of biological activities³⁹. For instance compounds (A) and (B) show antibacterial activity^{40–42}, compound (C) and (D) have anticancer activity^{43,44}, compound (E) shows anti-cholinesterase activity⁴⁵, compound (F) shows anti-inflammatory activity⁴⁶, compound (G) shows anti-fungal activity⁴⁷, compound (H) shows anti-viral activity⁴⁸, and compound (I) shows anti-oxidant activity⁴⁹ (Fig. 1). Knowing the biological importance of Schiff bases, this study focuses on synthesizing novel Schiff base derivatives as potent inhibitors of α -glucosidase. These synthetic compounds are expected to possess high lipophilicity, enhanced activity, and facilitating easy passage through cellular barriers.

Most of the synthetic anti-diabetic drugs are widely used now days because they are synthesized from cheaper reagent and are effective and safer than most of natural anti-diabetic drugs. On the basis of literature survey, the current research work is focused mainly on the synthesis of 3,4-dihydroxyphenylacetic acid derived Schiff bases, their molecular docking study and their α -glucosidase inhibition assay.

In the current work a series of 3,4-dihydroxyphenylacetic acid Schiff bases (1–28) were synthesized in good yields through multi-step reactions (Scheme 1). First 3,4-dihydroxyphenylacetic acid (a) was esterified to the corresponding esters (b) in ethanol and a small amount of sulfuric acid and then treated with excess amount of hydrazine hydrate to afford 3,4-dihydroxyphenylhydrazide (c). Subsequently, Schiff bases of 3,4-dihydroxyphenylhydrazide were obtained by treating c with various aromatic aldehydes in ethanol and catalytic amount of glacial acetic acid. All the Schiff bases were recrystallized from ethanol in good yields (1–28). The synthesized

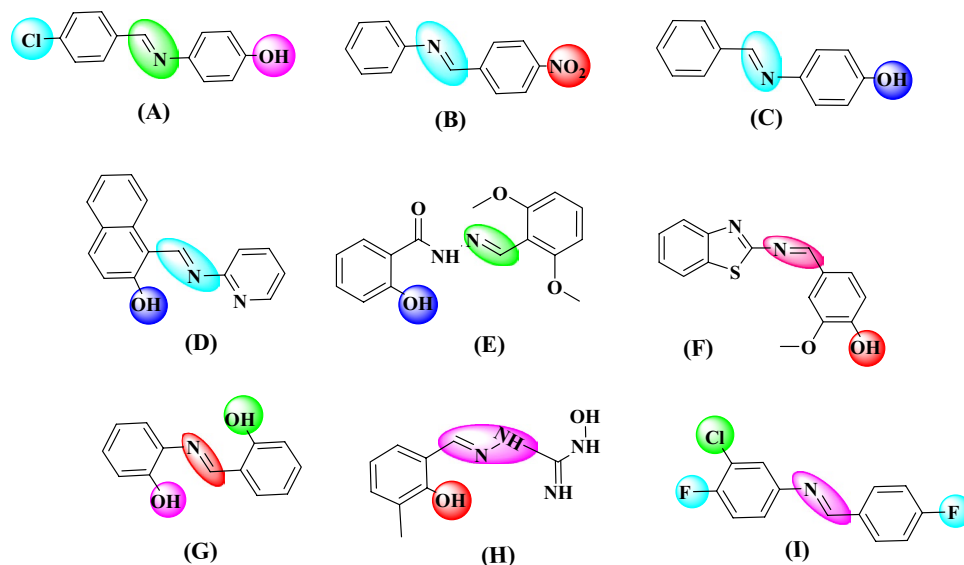
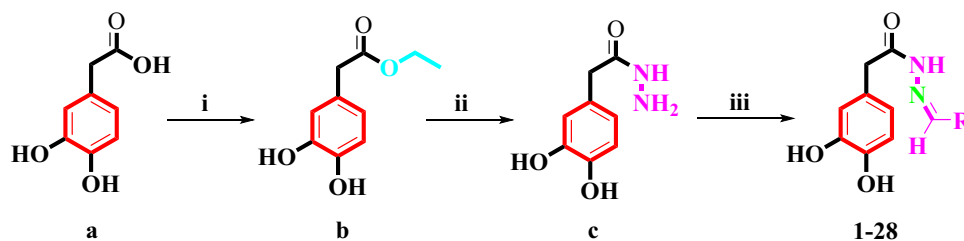


Figure 1. Commercially available drugs containing Schiff base moities.



- i. Conc H_2SO_4 (98%), EtOH, reflux
- ii. Hydrazine hydrate (80%), EtOH, reflux
- iii. Glacial AcOH, aromatic aldehydes, EtOH

Scheme 1. Design for the synthesis of Schiff bases of 3,4-dihydroxyphenylhydrazide.

Schiff bases were characterized with the help of $^1\text{H-NMR}$, $^{13}\text{C-NMR}$, and HR-ESI-MS spectroscopy. Finally, Schiff bases of 3,4-dihydroxyphenylhydrazide were subjected to α -glucosidase inhibition assay.

Materials and methods

3,4-Dihydroxyphenylacetic acid, hydrazine hydrate, ethanol, DMSO, potassium carbonate, and iodine were obtained from Macklin Company and used without further purification. Reactions were tracked using Merck aluminum TLC plates with 0.2 mm of silica gel 60 F-254. The $^1\text{H-NMR}$ and $^{13}\text{C-NMR}$ spectra of the synthesized compounds were recorded in DMSO- d_6 using an Avance Bruker AM 600 MHz spectrometer. Chemical shift values are expressed in ppm, and coupling constants (J) are reported in hertz (Hz). The molecular masses of the synthesized compounds were determined by high-resolution electrospray ionization mass spectrometry (HR-ESI-MS). Melting points of all the new synthesized compounds were determined using a Digital Electro-thermal apparatus.

Synthesis of ethyl 2-(2,4-dihydroxyphenyl)acetate (b)

In a 100 mL round-bottom flask, 3,4-dihydroxyphenylacetic acid (a) (1.68 g, 10 mmol) was dissolved in 35 mL of absolute ethanol. The temperature of this solution was lowered to 0 °C using an ethanol–water ice bath. Subsequently, 0.5 mL of concentrated sulfuric acid (H_2SO_4) was added drop wise as a dehydrating agent, and the mixture was stirred at room temperature for 2 h before being refluxed for an additional 8 h. After cooling the reaction mixture to room temperature, it was poured onto a beaker containing 20 mL of crushed ice. The esterified product (monitored via TLC) was collected through filtration and neutralized with a 5% aqueous solution of sodium bicarbonate (NaHCO_3), yielding 1.79 g of ethyl 2-(3,4-dihydroxyphenyl)acetate (b).

Synthesis of 2-(3,4-dihydroxyphenyl)acetohydrazide (c)

Ethyl 2-(3,4-dihydroxyphenyl)acetate (b) (0.98 g, 5 mmol) was dissolved in 10 mL of absolute ethanol, and 15 mmol of 80% hydrazine hydrate was gradually added. The reaction mixture was refluxed for 8–10 h, monitored by TLC using a solvent system of n-hexane and ethyl acetate (1:2). Upon completion of the reaction, the mixture was cooled to room temperature, resulting in the appearance of a precipitate. The precipitate was filtered, washed with an excess of distilled water (100 mL), and then dried in an oven set at 50 °C, yielding 0.87 g of the desired product (c).

Synthesis of Schiff bases (1–28)

One millimole of 3,4-dihydroxyphenylacetic acid hydrazide was subjected to a reaction with an equimolar amount of aromatic aldehyde in the presence of 5 mL of absolute ethanol as a solvent and a few drops of glacial acetic acid as catalyst. The reaction mixture was refluxed and allowed to stir overnight, with monitoring through TLC (ethyl acetate: n-hexane: methanol 1:1:0.5). The resulting precipitate was cooled to room temperature, filtered, dried, and subsequent recrystallization from ethanol afforded Schiff bases (1–28). The structural characterization of the synthesized Schiff bases was conducted through $^1\text{H-NMR}$, $^{13}\text{C-NMR}$, and HR-ESI-MS spectroscopy.

Results and discussions

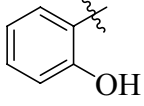
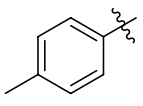
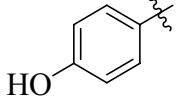
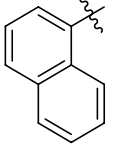
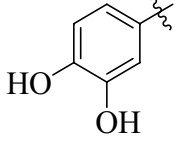
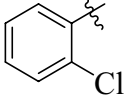
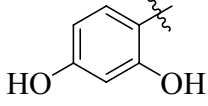
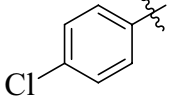
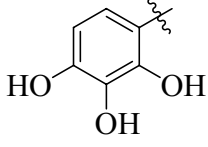
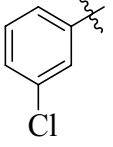
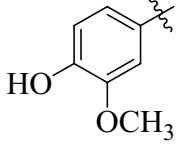
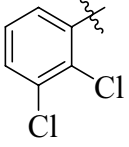
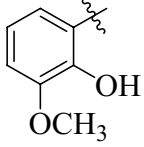
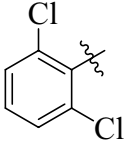
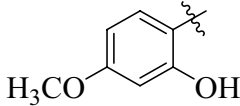
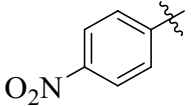
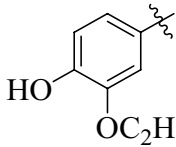
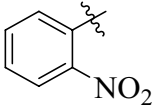
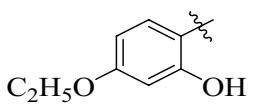
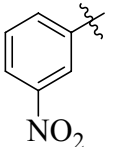
In vitro α -glucosidase inhibition effect

All synthetic novel Schiff bases of 3,4-dihydroxyphenylacetic acid derivatives (1–28) were subjected to α -glucosidase inhibition effect according to the literature protocol⁵⁰. Except compounds 22, 26, 27, and 28, all derivatives show good to moderate α -glucosidase inhibition potential ranging from ($\text{IC}_{50} = 12.84 \pm 0.52$ – 43.76 ± 2.34 μM) as compared to standard acarbose ($\text{IC}_{50} = 873.34 \pm 1.67$ μM). Compounds, 12 ($\text{IC}_{50} = 15.73 \pm 0.71$ μM), 15 ($\text{IC}_{50} = 17.40 \pm 0.74$ μM), 7 ($\text{IC}_{50} = 19.68 \pm 0.82$ μM), 4 ($\text{IC}_{50} = 13.64 \pm 0.58$ μM), 13 ($\text{IC}_{50} = 16.62 \pm 0.47$ μM), 2 ($\text{IC}_{50} = 20.35 \pm 1.27$ μM), 3 ($\text{IC}_{50} = 18.45 \pm 1.21$ μM) and 5 ($\text{IC}_{50} = 12.84 \pm 0.52$ μM) were found to be more potent among the series Table 1.

Structure–activity relationship (SAR)

Structure activity relation for α -glucosidase inhibition potential was developed from Table 1 by analyzing the effect of various aldehyde substituents, R and data of inhibition of the most active compounds as shown in Fig. 2. α -glucosidase inhibition activity of hydroxyl-substituted analogs (1–5) provides valuable insights into structure–activity relationships (SAR), with a focus on the positional effect of hydroxy groups. All derivatives showed excellent inhibition effect, among the analogs tested, the ortho-hydroxy analog 1 exhibited an excellent inhibition activity, with an IC_{50} value of 24.37 ± 0.83 , indicating a potential role for hydroxyl substitution at ortho position. Similarly, the para-hydroxy analog 2 demonstrated comparable activity, with an IC_{50} value of 20.35 ± 1.27 , suggesting that hydroxyl substitution at para position also contributes to inhibition potency. The introduction of a second hydroxyl group at positions meta and para position of compound 3 yielded a slightly increased inhibition activity, with an IC_{50} value of 18.45 ± 1.21 , highlighting the importance of the proximity and arrangement of hydroxyl groups. Further examination of another ortho, para dihydroxy analog 4 revealed a notable augmentation in inhibition activity, with an IC_{50} value of 13.64 ± 0.58 . Most notably, the ortho, meta, and para trihydroxy analog exhibited the highest inhibition activity among the hydroxyl substituted analogs tested, with an IC_{50} value of 12.84 ± 0.52 . However, it is crucial to note that all analogs displayed excellent inhibition activity compared to the standard inhibitor, acarbose, which had an IC_{50} value of 873.34 ± 1.67 .

Compounds 6–10 represent analogs where the hydrogen of one hydroxyl group has been substituted with either methoxy (compounds 6, 7, and 8) or ethoxy (compounds 9 and 10). The IC_{50} values for these analogs, namely 6 ($\text{IC}_{50} = 23.69 \pm 1.11$), 7 ($\text{IC}_{50} = 19.68 \pm 0.82$), 8 ($\text{IC}_{50} = 20.88 \pm 0.53$), 9 ($\text{IC}_{50} = 27.29 \pm 1.15$), and 10

Comp. No	R	IC ₅₀ ± SEM (μM)	Comp. No	R	IC ₅₀ ± SEM (μM)
1		24.37 ± 0.83	16		26.41 ± 1.10
2		20.35 ± 1.27	17		43.76 ± 2.34
3		18.45 ± 1.21	18		28.16 ± 1.09
4		13.64 ± 0.58	19		31.22 ± 1.40
5		12.84 ± 0.52	20		27.26 ± 0.83
6		23.69 ± 1.11	21		24.16 ± 0.52
7		19.68 ± 0.82	22		NA
8		20.88 ± 0.53	23		30.46 ± 1.28
9		27.29 ± 1.15	24		29.67 ± 0.98
10		28.66 ± 1.21	25		34.46 ± 1.48
Continued					

Comp. No	R	IC ₅₀ ± SEM (μM)	Comp. No	R	IC ₅₀ ± SEM (μM)
11		33.51 ± 1.22	26		NA
12		15.73 ± 0.71	27		NA
13		16.62 ± 0.47	28		NA
14		20.61 ± 0.59	Acarbose	Standard inhibitor	873.34 ± 1.67
15		17.405 ± 0.74			

Table 1. Results for different substituent attached to the products (1–28).

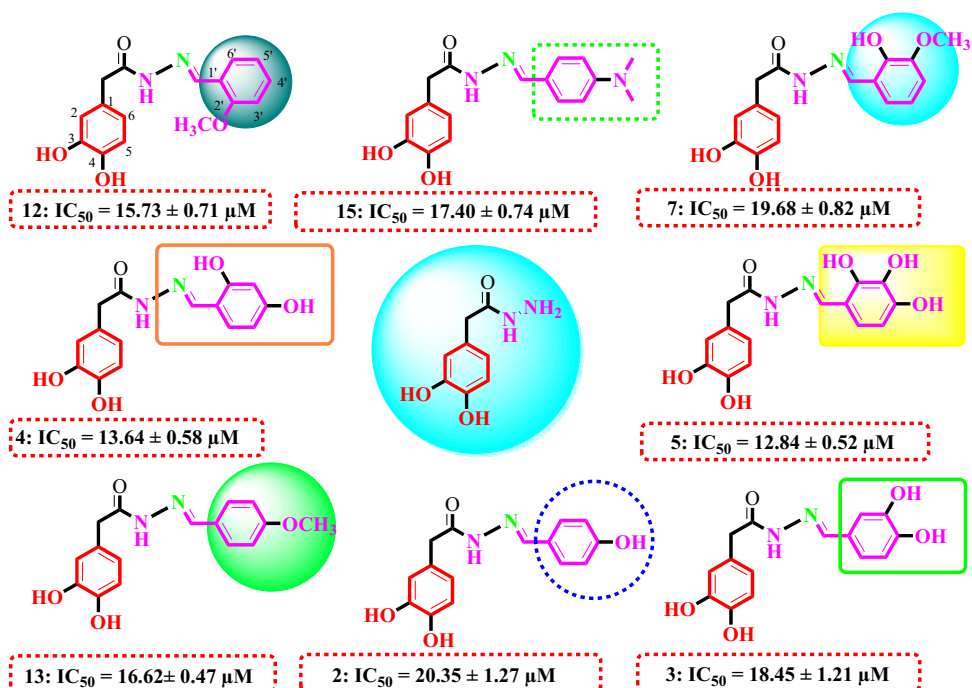


Figure 2. Structure Activity relationship of compounds 2, 3, 4, 5, 7, 12, 13, and 15.

($IC_{50} = 28.66 \pm 1.21$), indicate that the introduction of these electron-donating groups results in a slight decrease in inhibition activity. Moreover, the impact of the ethoxy group appears to be more pronounced than that of the methoxy group, as evidenced by the observed results. Compound **11**, featuring a hydroxyl group at the meta position and a methyl group at the para position, exhibited an IC_{50} value of 33.51 ± 1.22 , indicating a decrease in activity when compared to compounds **1–10**.

Compound **12**, with an IC_{50} of 15.73 ± 0.71 , is ortho-methoxy substituted, while compound **13**, with an IC_{50} of 16.62 ± 0.47 , is para-methoxy substituted. Compound **14**, an analog with meta, para-dimethoxy substitution, exhibits an IC_{50} of 20.61 ± 0.59 . Additionally, Compound **15**, featuring a para *N,N*-dimethylamino substituent, displays an IC_{50} of 17.405 ± 0.74 , while compound **16** (IC_{50} of 26.41 ± 1.10) and **17** (IC_{50} of 43.76 ± 2.34) with a methyl group at the para position and naphthalene respectively. The activity trends observed among these analogs underscore the significant role that both the position and nature of the substituent play in modulating inhibition activity.

Analogs **18–22** represent chloro-substituted variations. Analog **18** (ortho-chloro) exhibits an IC_{50} value of 28.16 ± 1.09 , analog **19** (para-chloro) shows an IC_{50} value of 31.22 ± 1.40 , and analog **20** (meta-chloro) demonstrates an IC_{50} value of 27.26 ± 0.83 . These analogs, each singly substituted with a chloro group, display no significant variation in activity based on the position of the chloro group. However, compound **21**, ortho meta dichloro-substituted, displays an enhanced activity with an IC_{50} value of 24.16 ± 0.52 , compared to its singly-substituted counterpart. Conversely, compound **22** ortho ortho dichloro-substituted, exhibits no inhibitory activity, indicating an extreme positional effect.

Analogs **23** (with an IC_{50} value of 30.46 ± 1.28), **24** (with an IC_{50} value of 29.67 ± 0.98), and **25** (with an IC_{50} value of 34.46 ± 1.48) represent para, ortho, and meta nitro-substituted variations, respectively. The inhibitory results of these analogs also suggest that the impact of the nitro group's position is relatively minor. Conversely, compounds **26–28** exhibited less than 50% inhibition, rendering them inactive.

In summary, the fundamental structure within this class of compounds predominantly dictates their activity. However, the specific characteristics of substituents within the structure exert a notable influence; for instance, hydroxyl substitutions, as well as those with electron-donating or electron-withdrawing properties, can either enhance or diminish the inhibitory activity. Moreover, introducing disubstitutions tends to amplify the effect on inhibition activity. Nonetheless, the positional arrangement of substituents appears to exert a relatively minor influence on inhibition activity.

Molecular docking

The docking study was carried out using the AutoDock Vina package (1.5.7 version)⁵¹. The docking study provides deep insight into synthesized compounds' binding modes with α -glucosidase. The protein structure of α -glucosidase was obtained from Protein Data Bank [<https://www.rcsb.org/structure/3WY1>]. The water molecules were eliminated from the protein structure, and the missing hydrogens were added to the protein structure using AutoDock Tools. For the docking calculations, a cube grid box was prepared with dimensions of 3.391, 1.310, and -8.362 Å in *x*, *y*, and *z*-directions. Furthermore, the grid box position was centered on the middle of compounds under docking. The AutoGrid Tools was used to form grid maps, and spacing within the grid was selected as 0.375 Å. The grid consists of 40 points along *x*, *y*, and *z*-directions. We focused on the amino acids that play a key role in the binding with the active site of targeted compounds, as we listed in Table 2.

The ligands (compounds) were made and optimized using the density functional theory (DFT) method. After the optimization, the ligands were used for docking calculation. The interactions between the ligands and amino acids of protein were visualized by the PyMOL 2.5.4. The visualization clearly shows the different types of interaction, such as van der Waals, attractive charges, conventional H-bonding, unfavorable interaction, and different types of π -interactions as shown in Fig. 3. The Biovia Discovery Studio was used for making the 2D representation of the interaction between protein and ligand.

The molecular docking analysis reveals complex interactions between compound **12** and various amino acid residues. In particular, THR.445, LYS.352, and ASN.46 engage in conventional hydrogen bonding with the oxo groups of the compound. On the other hand, ALA.45, ALA.451, LEU.433, ASN.447, and SER.44 form van der Waals interactions with the ligand. Additionally, HIS.348, ASP.441, and ARG.450 exhibit π -interactions with

Comps	Binding affinity (kcal/mol)	Types of interactions		
		Conventional H-bonds	Van der Waals	π^{π} -interactions
2	-7.9	HIS.348, ARG.437, ASN.447, ASP.441, ALA.451	THR.445, GLY.438, LEU.433, PHE.455, GLU.432, ALA.514, VAL.513, ASN.443, THR.448	ARG.450, ALA.454
12	-7.5	THR.445, LYS.352, ASN.44	ALA.45, ALA.451, LEU.433, ASN.447, SER.44	ASP.441, ARG.450, ALA.444, HIS.348
14	-8.2	ASP.441	VAL.513, ALA.514, GLU.432, LEU.433, THR.445, HIS.348, ASN.46, SER.44, PHE.455, SER.458, GLN.438, ALA.444, ASN.443, GLN.439	ARG.450, ARG.437, ALA.451, ALA.454
15	-8.0	THR.445, GLU.432, GLU.438	LEU.446, LEU.433, LYS.352, ALA.514, ASN.443, ARG.437, ASN.46, ARG.450, SER.44	HIS.348, ASP.441, ALA.444, ALA.451, ALA.454

Table 2. Different types of interaction with binding affinity.

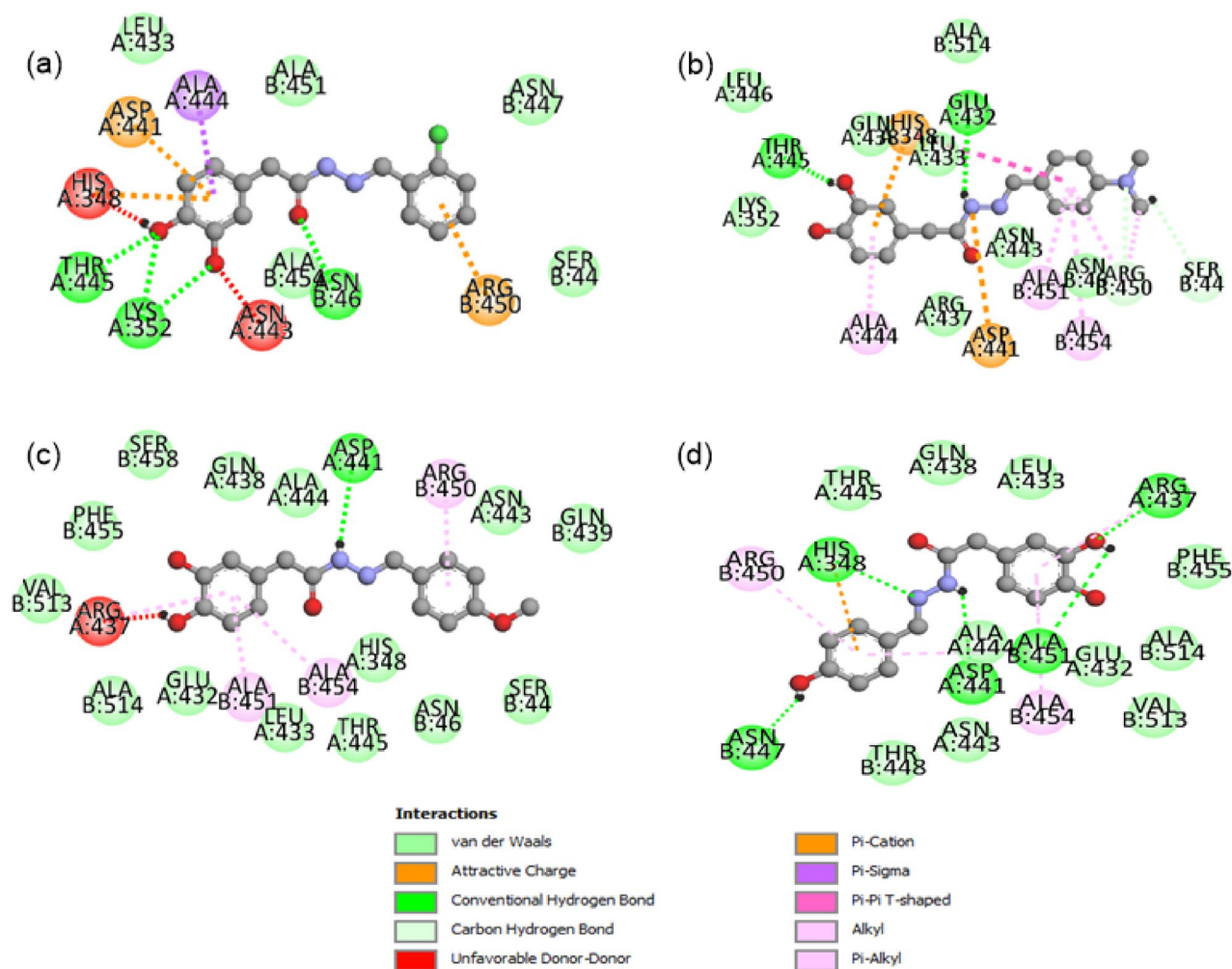


Figure 3. Docking studies of synthesized compounds 12, 15, 13, and 2, respectively.

the ring's delocalized electronic cloud, as shown in Table 2 and Fig. 3. Furthermore, ALA.444 reveals π -sigma bonding with the aromatic ring. Notably, HIS.348 and ASN.443 contribute to unfavorable interactions with the ligand's oxo groups. The overall binding affinity of compound 12 is calculated as -7.5 kcal/mol.

Compound 15, shows a higher binding affinity of -8.0 kcal/mol. This higher affinity reflects a substantial increase in the number of amino acid residues engaged in the interaction. Noteworthy contributors include LEU.446, LEU.433, LYS.352, ALA.514, and ASN.443, indicating their significant involvement through van der Waals interactions. Key amino acids, namely THR.445, LYS.352, and ASN.46, establish conventional hydrogen bonds with the OH and NH groups. The HIS.348 and ASP.441 participate in π -electronic interactions with the aromatic ring and NH through attractive charges/ π -cation interactions, as shown in Fig. 3. Furthermore, ALA.444, ALA.451, and ALA.454 contribute through π -alkyl interactions.

Compound 13 exhibits the highest binding affinity as -8.2 kcal/mol. Notably, conventional hydrogen bonding is reduced, with only ASP.441 forming such bonds with the NH group of synthesized compound. In contrast, van der Waals interactions significantly increase compared to other compounds, with noteworthy contributions from amino acids such as VAL.513, ALA.514, GLU.432, LEU.433, and others, as listed in Table 2. Furthermore, the ARG.450, ARG.437, ALA.451, and ALA.454 engage in π -interactions with the aromatic ring. These interactions highlight the unique binding characteristics of Compound 13.

Compound 2 shows the binding affinity as -7.9 kcal/mol. Notably, in Compound 2, an increased number of amino acids, including HIS.348, ARG.437, ASN.447, ASP.441, and ALA.451, actively contribute through conventional H-bonding. The engagement of oxygen and nitrogen atoms from compound 2 in H-bonding is shown in Fig. 3. The multifaceted role of HIS.348 not only participates in conventional hydrogen bonding but also engages in π -cation interactions with the aromatic ring. Furthermore, Compound 2 is surrounded by many amino acids through van der Waals interactions, as detailed in Table 2. Additionally, ARG.450 and ALA.454 contribute through π -interactions. After an in-depth molecular docking analysis, compounds 12, 15, 13, and 2 exhibited diverse interaction profiles with the target protein. These findings underscore their unique binding characteristics, providing valuable insights for their potential development as promising drug discovery and optimization candidates.

Conclusion

A series of novel Schiff base derivatives (1–28) of 3,4-dihydroxyphenylacetic acid were successfully synthesized and characterized using advanced spectroscopic techniques, including ¹H-NMR, ¹³C-NMR, and high-resolution electrospray ionization mass spectrometry (HR-ESI-MS). Subsequently, the inhibitory potential of these compounds against the α-glucosidase enzyme was evaluated. Most of our synthesized compounds exhibited satisfactory to moderate inhibitory activity against α-glucosidase (see Supplementary information). Notably, derivatives 12, 15, 7, 4, 13, 2, 3, and 5 demonstrated outstanding inhibition, showcasing IC₅₀ values ranging between 12.84 ± 0.52 μM and 20.35 ± 1.27 μM. To further elucidate the binding modes of these promising derivatives with the enzyme active site, molecular docking studies were conducted. This comprehensive approach provides valuable insights into the synthesized compounds' inhibitory potential and their potential application in developing α-glucosidase inhibitors.

Data availability

All data generated or analysed during this study are included in this published article and its supplementary information files.

Received: 24 December 2023; Accepted: 13 May 2024

Published online: 18 May 2024

References

1. Khunti, K. *et al.* Diabetes and multiple long-term conditions: A review of our current global health challenge. *Diabetes Care* **46**, 2092–2101 (2023).
2. Durmaz, L. *et al.* Screening of carbonic anhydrase, acetylcholinesterase, butyrylcholinesterase, and α-glucosidase enzyme inhibition effects and antioxidant activity of coumestrol. *Molecules* **27**, 3091 (2022).
3. Cakmak, K. C. & Gülçin, İ. Anticholinergic and antioxidant activities of usnic acid—an activity-structure insight. *Toxicol. Rep.* **6**, 1273–1280 (2019).
4. Durmaz, L. *et al.* Antioxidant, antidiabetic, anticholinergic, and antiglaucoma effects of magnofluorine. *Molecules* **27**, 5902 (2022).
5. Mathews, A. S. M. *et al.* Impact of diabetes on cardiovascular disease: An update. *Int. J. Hypertens.* **2013**, 1–15. <https://doi.org/10.1155/2013/653789> (2013).
6. Yi, J. *et al.* Polypeptide from moschus suppresses lipopolysaccharide-induced inflammation by inhibiting NF-κ B-ROS/NLRP3 pathway. *Chin. J. Integr. Med.* **29**, 895–904 (2023).
7. Toeller, M. α-Glucosidase inhibitors in diabetes: efficacy in NIDDM subjects. *Eur. J. Clin. Invest.* **24**, 31–35 (1994).
8. Cui, G. *et al.* Synthesis and characterization of Eu (III) complexes of modified cellulose and poly (N-isopropylacrylamide). *Carbohydr. Polym.* **94**, 77–81 (2013).
9. Derosa, G. & Maffioli, P. α-Glucosidase inhibitors and their use in clinical practice. *Arch. Med. Sci. AMS* **8**, 899 (2012).
10. Wang, Y., Zhai, W., Cheng, S., Li, J. & Zhang, H. Surface-functionalized design of blood-contacting biomaterials for preventing coagulation and promoting hemostasis. *Friction* **11**, 1371–1394 (2023).
11. Zhang, B.-W. *et al.* Dietary flavonoids and acarbose synergistically inhibit α-glucosidase and lower postprandial blood glucose. *J. Agric. Food Chem.* **65**, 8319–8330 (2017).
12. Smith, D. L., Orlandella, R. M., Allison, D. B. & Norian, L. A. Diabetes medications as potential calorie restriction mimetics—a focus on the alpha-glucosidase inhibitor acarbose. *GeroScience* **43**, 1123–1133 (2021).
13. Wang, W. *et al.* Macrophage-derived biomimetic nanoparticles for light-driven theranostics toward Mpox. *Matter* **7**, 1187–1206 (2024).
14. Lin, A.H.-M., Lee, B.-H. & Chang, W.-J. Small intestine mucosal α-glucosidase: A missing feature of in vitro starch digestibility. *Food Hydrocoll.* **53**, 163–171 (2016).
15. Cui, G. *et al.* Synthesis and characterization of phenylboronic acid-containing polymer for glucose-triggered drug delivery. *Sci. Technol. Adv. Mater.* **21**, 1–10 (2020).
16. Bai, R. *et al.* Second generation β-element nitric oxide derivatives with reasonable linkers: Potential hybrids against malignant brain glioma. *J. Enzyme Inhib. Med. Chem.* **37**, 379–385 (2022).
17. Joshi, S. R. *et al.* Therapeutic potential of α-glucosidase inhibitors in type 2 diabetes mellitus: An evidence-based review. *Expert Opin. Pharmacother.* **16**, 1959–1981 (2015).
18. Leroux-Stewart, J., Rabasa-Lhoret, R. & Chiasson, J. L. α-Glucosidase inhibitors. In *International Textbook of Diabetes Mellitus*, 673–685 (2015).
19. Zhang, Y. *et al.* Ephedra Herb extract ameliorates adriamycin-induced nephrotic syndrome in rats via the CAMKK2/AMPK/mTOR signaling pathway. *Chin. J. Nat. Med.* **21**, 371–382 (2023).
20. Khan, M. *et al.* Synthesis, molecular modeling and biological evaluation of 5-arylidene-N, N-diethylthiobarbiturates as potential α-glucosidase inhibitors. *Med. Chem.* **15**, 175–185 (2019).
21. Zhao, J. *et al.* Tumor cell membrane-coated continuous electrochemical sensor for GLUT1 inhibitor screening. *J. Pharm. Anal.* **13**, 673–682 (2023).
22. Zhang, Z., Zhang, W., Hou, Z.-W., Li, P. & Wang, L. Electrophilic halospirocyclization of N-benzylacrylamides to access 4-halo-methyl-2-azaspiro [4.5] decanes. *J. Org. Chem.* **88**, 13610–13621 (2023).
23. Gul, S. *et al.* Synthesis, molecular docking and DFT analysis of novel bis-Schiff base derivatives with thiobarbituric acid for α-glucosidase inhibition assessment. *Sci. Rep.* **14**, 3419 (2024).
24. Cui, G. *et al.* Synthesis and characterization of Eu (III) complexes of modified D-glucosamine and poly (N-isopropylacrylamide). *Mater. Sci. Eng. C* **78**, 603–608 (2017).
25. Jia, Y. & Li, J. Molecular assembly of Schiff base interactions: Construction and application. *Chem. Rev.* **115**, 1597–1621 (2015).
26. Jamil, W. *et al.* Phenoxyacetohydrazide Schiff bases: β-Glucuronidase inhibitors. *Molecules* **19**, 8788–8802 (2014).
27. Chen, H. & Rhodes, J. Schiff base forming drugs: Mechanisms of immune potentiation and therapeutic potential. *J. Mol. Med.* **74**, 497–504 (1996).
28. Aziz, A. N. *et al.* Synthesis, crystal structure, DFT studies and evaluation of the antioxidant activity of 3, 4-dimethoxybenzenamine Schiff bases. *Molecules* **19**, 8414–8433 (2014).
29. Jamil, W. *et al.* Synthesis, anti-diabetic and in silico QSAR analysis of flavone hydrazide Schiff base derivatives. *J. Biomol. Struct. Dyn.* **40**, 12723–12738 (2022).
30. Yiğit, B., Yiğit, M., Taslimi, P., Gök, Y. & Gülçin, İ. Schiff bases and their amines: Synthesis and discovery of carbonic anhydrase and acetylcholinesterase enzymes inhibitors. *Archiv Pharm.* **351**, 1800146 (2018).
31. Buldurun, K. *et al.* Synthesis, characterization, powder X-ray diffraction analysis, thermal stability, antioxidant properties and enzyme inhibitions of M (II)-Schiff base ligand complexes. *J. Biomol. Struct. Dyn.* **39**, 6480–6487 (2021).

32. Aytac, S., Gundogdu, O., Bingol, Z. & Gulcin, I. Synthesis of Schiff bases containing phenol rings and investigation of their antioxidant capacity, anticholinesterase, butyrylcholinesterase, and carbonic anhydrase inhibition properties. *Pharmaceutics* **15**, 779 (2023).
33. Da Silva, C. M. *et al.* Schiff bases: A short review of their antimicrobial activities. *J. Adv. Res.* **2**, 1–8 (2011).
34. Sykula, A. D. A. Schiff bases as important class of pharmacological agents. *J. Pharm. Pharmacol.* **6**, 989–1009 (2018).
35. Khan, M. *et al.* Synthesis of new bis (dimethylamino) benzophenone hydrazone for diabetic management: In-vitro and in-silico approach. *Heliyon* **10**, e23323 (2024).
36. Sahu, R. & Thakur, D. Schiff base: An overview of its medicinal chemistry potential for new drug molecules. *Int. J. Pharm. Sci. Nanotechnol. (IJPSN)* **5**, 1757–1764 (2012).
37. Xu, W.-X. *et al.* Personalized application of antimicrobial drugs in pediatric patients with augmented renal clearance: a review of literature. *European Journal of Pediatrics*, 1–10 (2023).
38. Riaz, M. *et al.* Unraveling the molecular structure, spectroscopic properties, and antioxidant activities of new 2, 4-dinitrophenyl-hydrazone derivatives through a comprehensive investigation. *Arabian Journal of Chemistry* **16**, 105259 (2023).
39. Khan, M. *et al.* Green synthesis, characterization, DPPH and ferrous Ion-chelating (FIC) activity of Tetrakis-Schiff's bases of terephthalaldehyde. *Lett. Drug Design Discov.* **16**, 249–255 (2019).
40. Durgun, M. *et al.* Synthesis, characterisation, biological evaluation and in silico studies of sulphonamide Schiff bases. *J. Enzyme Inhib. Med. Chem.* **35**, 950–962 (2020).
41. Ashraf, M. A., Mahmood, K., Wajid, A., Maah, M. J. & Yusoff, I. Synthesis, characterization and biological activity of Schiff bases. *IPCBE* **10**, 185 (2011).
42. Xavier, A. & Srividhya, N. Synthesis and study of Schiff base ligands. *IOSR J. Appl. Chem.* **7**, 06–15 (2014).
43. Sadia, M. *et al.* Schiff base ligand L synthesis and its evaluation as anticancer and antidepressant agent. *J. King Saud Univ. Sci.* **33**, 101331 (2021).
44. Suyambulingam, J. K. *et al.* Synthesis, structure, biological/chemosensor evaluation and molecular docking studies of aminobenzothiazole Schiff bases. *J. Adhes. Sci. Technol.* **34**, 2590–2612 (2020).
45. Raza, R. *et al.* Synthesis and biological evaluation of 3-thiazolocoumarinyl schiff-base derivatives as cholinesterase inhibitors. *Chem. Biol. Drug Design* **80**, 605–615 (2012).
46. Liaras, K., Fesatidou, M. & Geronikaki, A. Thiazoles and thiazolidinones as COX/LOX inhibitors. *Molecules* **23**, 685 (2018).
47. El-Tabl, A. S., Shakhofa, M. M., El-Seidy, A. M. & Al-Hakimi, A. N. Synthesis, characterization and antifungal activity of metal complexes of 2-(5-((2-chlorophenyl) diazenyl)-2-hydroxybenzylidene) hydrazinecarbothioamide. *Phosphorus Sulfur Silicon Relat. Elem.* **187**, 1312–1323 (2012).
48. Kumar, K. S., Ganguly, S., Veerasamy, R. & De Clercq, E. Synthesis, antiviral activity and cytotoxicity evaluation of Schiff bases of some 2-phenyl quinazoline-4 (3) H-ones. *Eur. J. Med. Chem.* **45**, 5474–5479 (2010).
49. Mermer, A. *et al.* Synthesis of novel Schiff bases using green chemistry techniques; antimicrobial, antioxidant, antiurease activity screening and molecular docking studies. *J. Mol. Struct.* **1181**, 412–422 (2019).
50. Pierre, C., Roland, R., Tremblay, R. & Dube, J. p-Nitrophenol- α -D-glucopyranoside as substrate for measurement of maltase activity in human semen. *Clin. Chem.* **24**, 208–211 (1978).
51. Trott, O. & Olson, A. J. AutoDock Vina: Improving the speed and accuracy of docking with a new scoring function, efficient optimization, and multithreading. *J. Comput. Chem.* **31**, 455–461 (2010).

Acknowledgements

Authors are thankful to researchers supporting project number (RSP2024R235), King Saud University, Riyadh, Saudi Arabia.

Author contributions

H.K. synthesized the compounds, while H.K., A.A., F.A., and M.K. performed structural elucidation and wrote the original draft of the manuscript. A.K., S.U., and A.A performed the α -glucosidase inhibitory activity of the compounds. F.J. and A.S. performed molecular docking study of the synthesized compounds. M.K. and S.A. designed and supervised the project, assisted in the writing, the reviewing, and the editing of the manuscript. All authors have read and agreed to the published version of the manuscript.

Competing interests

The authors declare no competing interests.

Additional information

Supplementary Information The online version contains supplementary material available at <https://doi.org/10.1038/s41598-024-62034-x>.

Correspondence and requests for materials should be addressed to A.A.-H., M.K. or S.A.

Reprints and permissions information is available at www.nature.com/reprints.

Publisher's note Springer Nature remains neutral with regard to jurisdictional claims in published maps and institutional affiliations.



Open Access This article is licensed under a Creative Commons Attribution 4.0 International License, which permits use, sharing, adaptation, distribution and reproduction in any medium or format, as long as you give appropriate credit to the original author(s) and the source, provide a link to the Creative Commons licence, and indicate if changes were made. The images or other third party material in this article are included in the article's Creative Commons licence, unless indicated otherwise in a credit line to the material. If material is not included in the article's Creative Commons licence and your intended use is not permitted by statutory regulation or exceeds the permitted use, you will need to obtain permission directly from the copyright holder. To view a copy of this licence, visit <http://creativecommons.org/licenses/by/4.0/>.

© The Author(s) 2024